Jet Trajectories and Surface Pressures Induced on a Body of Revolution with Various Dual Jet Configurations

J. A. Schetz* and A. K. Jakubowski†
Virginia Polytechnic Institute and State University, Blacksburg, Virginia
and
K. Aoyagi‡
NASA Ames Research Center, Moffett Field, California

A jet in a crossflow is of interest in practical situations, including jet-powered VTOL aircraft. Three aspects of the problem have received little prior study: the effect of the angle of the jet to the crossflow, performance of dual-jet configurations, and a jet injected from a body of revolution as opposed to a flat plate. This work was designed to address these three aspects. The experiments were conducted in the 7×10 tunnel at NASA Ames at velocities from 14.5 to 35.8 m/s (47.6 to 117.4 ft/s). Detailed pressure distributions are presented for single and dual jets over a range of velocity ratios from 3 to 8, spacings from 2 to 6 diameters, and injection angles of 90, 75, and 60 deg. Some flowfield measurements are also presented, and it is shown that a simple analysis is capable of predicting the trajectories of the jets.

Nomenclature

C_p = pressure coefficient
ΔC_p = pressure coefficient difference ($C_{p_{\text{jet on}}} - C_{p_{\text{jet off}}}$)
D = diameter
$\dot{m}$ = mass flow rate
M = Mach number
P = pressure
q = dynamic pressure
R = nominal velocity ratio
S = center to center jet spacing
T = temperature
V = velocity
x = streamwise coordinate measured from center of the front nozzle
X = x/D
y = transverse coordinate (arc length for body of revolution) measured from nozzle center; plus (+) is to the right looking downstream
Y = y/D
ρ = density
θ = injection angle measured from the horizontal
δ^* = boundary layer displacement thickness

Subscripts and Superscript

b = main body
j = jet conditions
∞ = freestream conditions
$(\bar{\ })$ = averaged quantity over jet exit

Introduction

THE flowfield produced by a jet in a crossflow is of interest in a number of practical situations ranging from smokestacks and powerplant and sewage outfalls to jet-powered VTOL aircraft. The available information on this flow, in general, is discussed in Ref. 1. For the VTOL application, the pressure field induced on adjacent surfaces is of particular importance. Thus, there have been a number of detailed experimental studies of that part of the flowfield (see Refs. 2-12). Reviews of the early work can be found in Refs. 13 and 14, and an up-to-date tabulation of the available information in Ref. 15. The jet generally induces negative (with respect to the freestream) pressures on the nearby surfaces, and this results in a net loss of lift on the body. The longitudinal variation of the surface pressures is also important, since that determines the pitching moment.

There are three aspects of the general problem that have received little or no careful previous study. The first is the effect of the angle of the jet to the crossflow. That is important because the transition to wingborne operation is commonly accompanied by a change in the angle of the jet

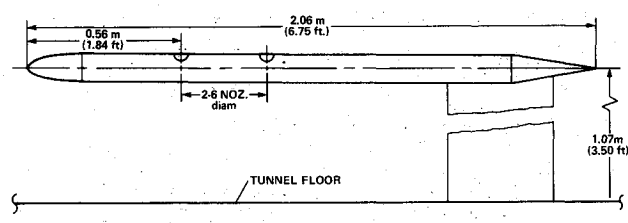

a) Dimensioned sketch of complete model.

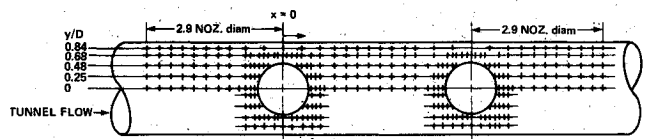

b) Plan view with pressure tap layout.

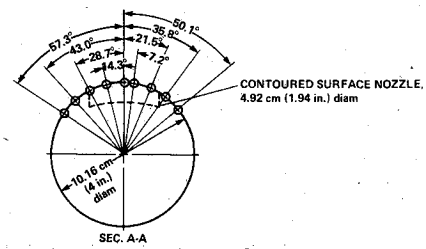

c) End view with pressure tap layout.

Fig. 1 Body of revolution wind tunnel model.

Presented as Paper 83-0080 at the AIAA 21st Aerospace Sciences Meeting, Reno, Nev., Jan. 10-13, 1983; received Jan. 28, 1983; revision received April 20, 1983.

*Professor and Dept. Chairman. Associate Fellow AIAA.
†Associate Professor. Member AIAA.
‡Aerospace Engineer. Member AIAA.

thrust vector. There are few prior investigations (see Refs. 8, 11, and 16). The second item is the performance of dual-jet configurations. The mutual interference as a function of center-to-center spacing is the issue here. Again, few references (e.g., Refs. 3, 8, and 17) exist. The third item for further study is the behavior of a jet (or jets) injected from a body of revolution as opposed to the flat plates usually considered. This is of obvious importance for VTOL aircraft with lifting jets in the fuselage. One can anticipate substantial transverse pressure "relief" around a cylindrical body. The only previous work found is Ref. 18, which considered a case where $D_{jet}/D_{body} \ll 1$. That is not realistic for VTOL aircraft where $D_{jet}/D_{body} \approx \frac{1}{2}$ can be encountered. Finally, the interplay of the three items mentioned here over a range of the key parameter for all such flows, V_{jet}/V_{stream}, is clearly of importance.

There have also been a number of analyses and semiempirical analyses for the jet in a crossflow problem (e.g., Refs. 15 and 19-28). None of them, however, can presently treat in a fundamental way the combination of two or more of the three items selected here for study. It is hoped that the experimental studies reported herein will aid in the generalization of the existing analyses.

The test plan was designed to provide new information on the influence of the three effects chosen: 1) injection angle, 2) multiple jets, and 3) a body of revolution with $D_{jet}/D_{body} \approx \frac{1}{2}$.

Apparatus

Facility

The experiments were conducted in the 7×10 ft (2.13×3.05 m) Subsonic Wind Tunnel at the NASA Ames Research Center at velocities from 14.5 to 35.8 m/s (47.6 to 117.4 ft/s), depending upon the jet/freestream velocity ratio desired. This facility is described in Ref. 29.

Test Models

The body of revolution model is shown in Fig. 1. The front jet nozzle is always located 0.56 m (1.84 ft) from the nose; the rear nozzle is shifted axially to achieve the various jet spacings considered.

Each nozzle is located in a 10.16 cm (4.0 in.) long section that is made from a 10.16 cm (4.0 in.) diameter tube split in half longitudinally. There are a number of spacer sections either 5.08 or 10.16 cm (2.0 or 4.0 in.) long to occupy the areas ahead of, between, and behind the nozzle sections in the arrangements for the various jet spacings. The jets had a 4.92 cm (1.94 in.) exit diameter to give $D_{jet}/D_{body} \approx \frac{1}{2}$.

On the basis of previous studies of the pressure field near the exhaust, detailed coverage of the model surface with pressure taps was clearly necessary. Preliminary layouts indicated that as many as 2000 pressure taps would be required for this two-jet arrangement. That implied not only excessive instrumentation requirements but prohibitive problems with running the pressure leads out through the body. Thus, it was decided to utilize the presumed right/left symmetry of the flow and locate pressure taps on an asymmetric pattern. Some redundant locations were incorporated to enable checks on the right/left symmetry of the pressure field. Finally, the pressure tap layout was designed with closer spacing in the immediate vicinity of the jets. The final configuration for the 90 deg injectors is shown in Fig. 1b. They are laid out on a grid with values of x/D indicating axial location with respect to the center of the front jet and values of y/D indicating arc distance off the centerline of the jets. The layout of the spacers was on a simpler pattern, as can be seen in Fig. 1b, which is for the six-jet-diameter spacing arrangement.

The boundary layer on the body was measured at a station in line with the back of the front nozzle at speeds corresponding to 1.0-5.0 cm H_2O (12.7-28.5 m/s) which covered the lower half of the test range. The displacement thickness was found to vary from 0.091 cm at the lower speed to 0.067 cm at the higher. These values indicate $\delta^*/D_{jet} \approx 1/50$, which must be considered in the small boundary-layer range. The velocity profiles indicated turbulent flow. At the lowest speed in the test plan, the Reynolds number based on the length to the center of the front nozzle is 5.6×10^5.

Injector Design

The requirement for $D_{jet}/D_{body} \approx \frac{1}{2}$ caused difficult problems in the design of the jet injectors. It was desired to have a relatively uniform jet exit velocity profile for all injection angles. Nonuniformities in jet exit profiles have been shown to influence the surface pressure field.[12]

Good exit profiles were obtained with the injector design finally chosen, illustrated for the 90 deg injector in Fig. 2. The air supply is via four tubes that entered the bottom. These lines fed passages that exited into the plenum chamber from four round vents in the bottom. The air left the vents through four holes around the periphery of each. This configuration was selected in an attempt to distribute the entering flow over the cross section of the necessarily short (in the flow direction) plenum. Just above the vent exits is a perforated plate with the hole pattern shown which serves as the next step in the flow distribution process. This hole pattern was refined by trial and error, and different patterns were required for the other injection angles. The flow straightener insert, shown in section C-C, consists of a tube holding a honeycomb with screening on the top and bottom. Finally, two types of jet exit geometry were considered, and they were accomplished by having two different flow straightener sections for each nozzle. The first type had a curved exit to match the contour of the body. The second was flat and flush with the highpoint of the body surface.

Instrumentation

The primary instrumentation for all the tests was a group of 48-port Scanivalves. The integrity of each lead from every pressure tap was carefully checked by applying a known pressure to the tap at the model surface and reading the output from the Scanivalve. The Scanivalves were operated and the data were obtained from them interactively by the recently developed data acquisition system for the 40×80 and 7×10 wind tunnels at Ames Research Center. All of the data were recorded on tape for subsequent data reduction. A three dimensional yaw head probe was used to obtain measurements in the plumes of some jets. Mean velocity, flow angularity, and static pressure profiles in the jets were obtained with this probe. The calibration curves for this probe, which are presented in Ref. 30, enabled the various mean flow

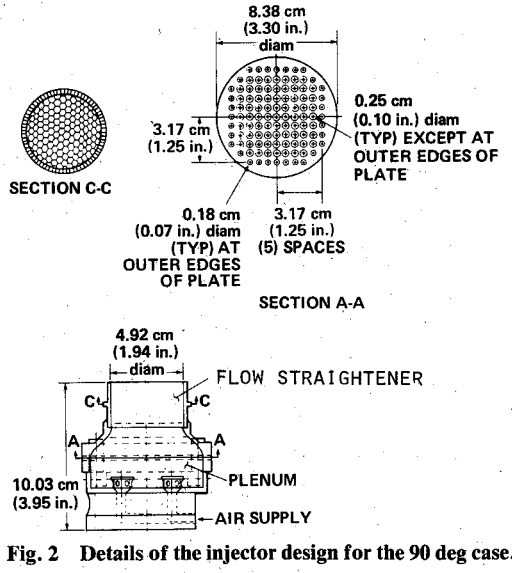

Fig. 2 Details of the injector design for the 90 deg case.

quantities to be determined over a wide range of angularity in any direction.

Test Plan

One could obtain the desired range of jet to freestream velocity ratios by a variety of paths, including holding the freestream velocity constant and varying the jet velocity, or vice versa. There is some appeal to testing at a constant freestream velocity, because that would keep the body Reynolds number and the boundary layer thickness constant. However, the difficulties and effort required to achieve uniform jet exit velocity profiles over a range in jet average velocity of 3:1 was judged to be so severe as to justify the choice of holding the jet velocity fixed and varying the freestream. As a check on the influence of the body Reynolds number variation thus introduced, one case at the same R but with a different freestream velocity was included for most configurations.

There were three other constraints that influenced the test plan. First, it was thought important to keep the minimum body Reynolds number based on the surface distance to the first nozzle above a certain value, picked as 5×10^5, to have a turbulent boundary layer. This meant a freestream velocity above roughly 13 m/s. Second, to avoid strong compressibility effects, it was decided to keep the maximum jet velocities below roughly 120 m/s ($M_j < 0.35$). Third, the pressure drop through the most severely inclined injectors was large enough to limit the mass flow (and thus the jet velocity) that could be obtained for those configurations.

Taking all of the items above into account, a test plan was adopted that had a nominal jet volume flow rate of 0.214 m^3/s, corresponding to $\bar{V}_j = 112.5$ m/s, and freestream velocities corresponding to $1.28 \le q \le 8.03$ cm H_2O ($14.5 \le V_\infty \le 35.8$ m/s).

Results

General

The data were reduced and the results are presented here as $\Delta C_p = (C_{p_{\text{jet on}}} - C_{p_{\text{jet off}}})$ as a function of spatial location on the body surface for each configuration. In this way, the first-order effects of any asymmetries or surface irregularities on the models should be normalized out. Before being accepted, each set of data was examined against some qualification criteria. The first group of these involved the jet injection conditions. Was the mass flow (and thus $\bar{V}_j$) set close enough to the desired nominal conditions? For the two-jet tests, were the mass flows close enough to each other? For these items, a tolerance of roughly ±5% was adopted. Next, when combined with the actual tunnel speed for a given data point, was the desired value of R achieved within again roughly ±5%? These questions were important, since we wished to make case-to-case comparisons such as the effect of jet spacing holding R nominally fixed, etc. The next examination of the acceptability of data centered on the right/left symmetry of the flow. For that purpose, the ΔC_p from the redundant ports at $x/D = 0.625$ and 0.875 to the right and left were compared. Here, it was found necessary to adopt the cruder tolerance of ±15%.

The data are presented as plots of axial and transverse variations of ΔC_p. The axial plots are for $y/D = 0.0$, 0.480, 0.248, 0.682, and 0.842 for the body of revolution. The transverse plots are at different groups of values of x/D depending upon the jet spacing under test.

The results obtained for $R = 7.7$, 90 deg injection through nozzles with exits contoured to the body surface at a spacing of 2.0 diameters, are shown in Fig. 3 as open circles. The results obtained for injection from the front nozzle only with the exit of the rear nozzle carefully covered by tape are shown as the solid circles. That notational practice is followed throughout. Looking at the single-jet results first, the expected pattern of negative C_p is evident. The magnitude of the pressure coefficients near the injectors agrees with those found on flat plates. The influence of the round main body compared to a flat plate case is evidenced as a faster decay in the maximum ΔC_p with y/D, that is, perpendicular to the

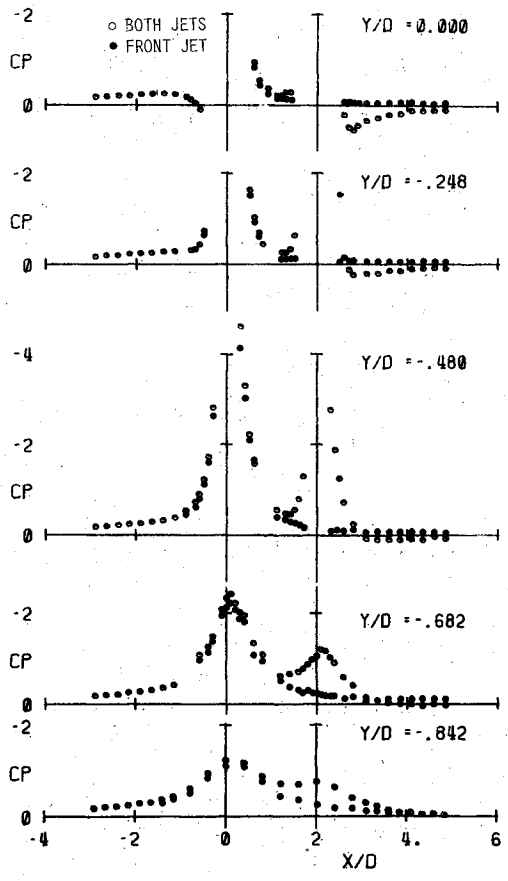

Fig. 3 Surface pressure distribution (ΔC_p): 90 deg, $R = 7.7$, $S/D = 2$, and contoured exit.

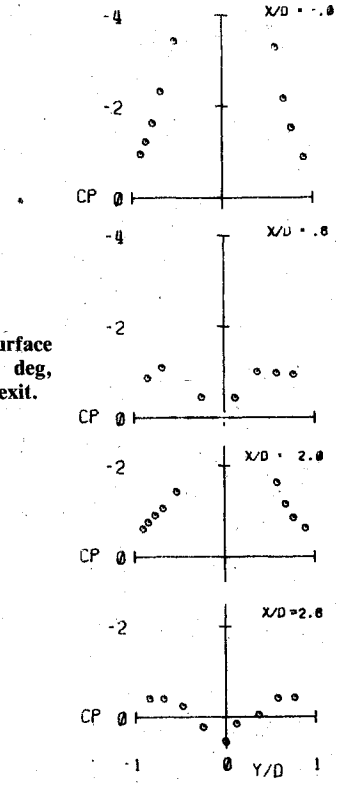

Fig. 4 Transverse plot of surface pressure distribution with 90 deg, $R = 7.7$, $S/D = 2$, and contoured exit.

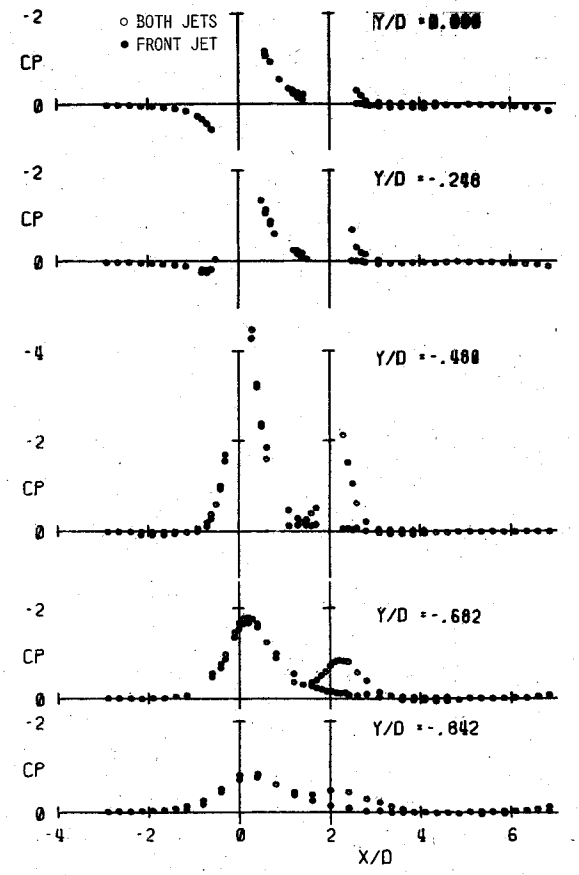

Fig. 5 Surface pressure distribution (ΔC_p): 90 deg, $R=3.2$, $S/D=2$, and contoured exit.

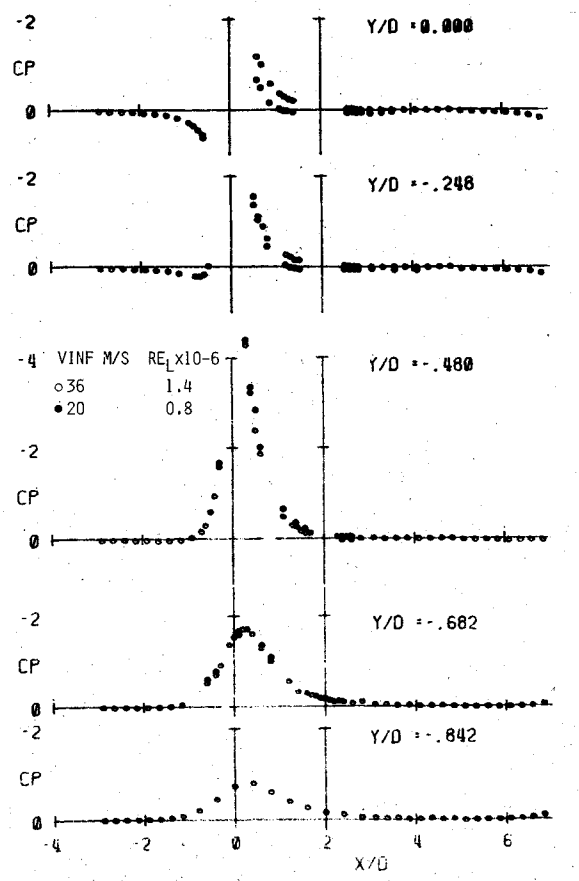

Fig. 6 Comparison of surface pressure distribution at the same $R=3.2$, but two different Re_L with 90 deg, $S/D=2$, and contoured exit. Front nozzle only.

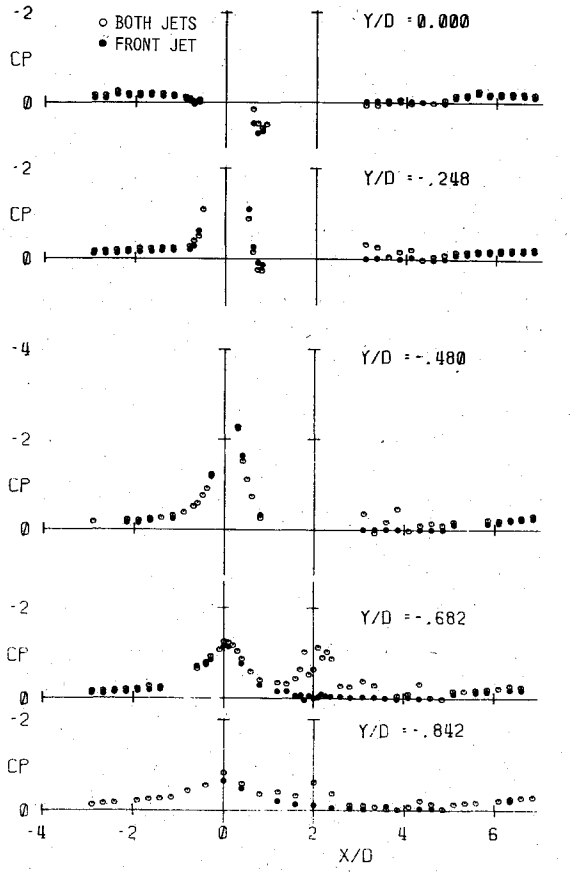

Fig. 7 Surface pressure distribution (ΔC_p): 90 deg, $R=8$, $S/D=2$, and flat-top exit.

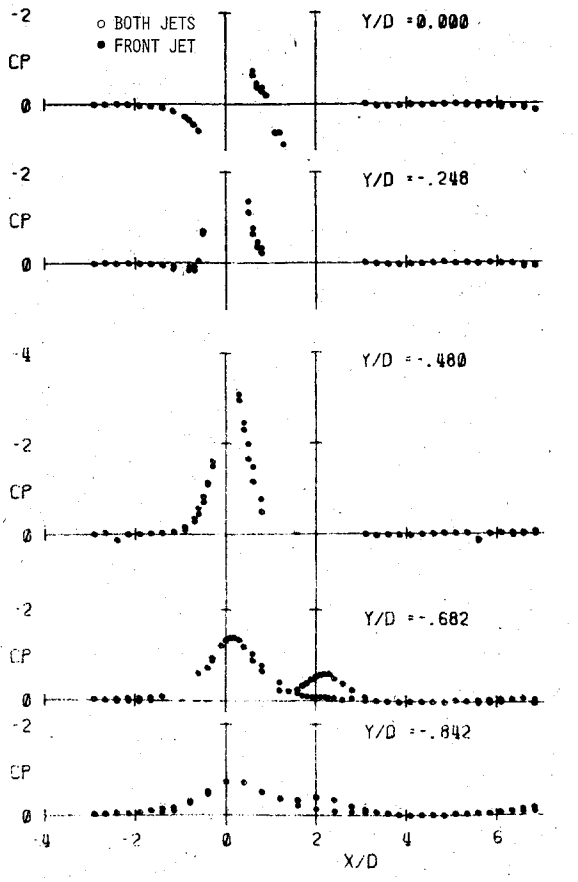

Fig. 8 Surface pressure distribution (ΔC_p): 90 deg, $R=3.3$, $S/D=2$, and flat-top exit.

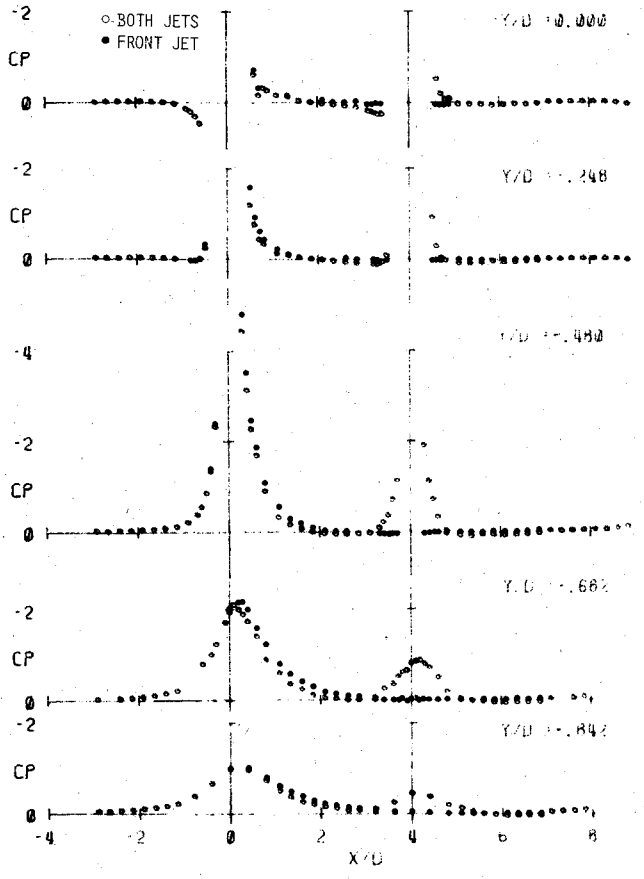

Fig. 9 Surface pressure distribution (ΔC_p): 90 deg, $R=4.7$, $S/D=4$, and contoured exit.

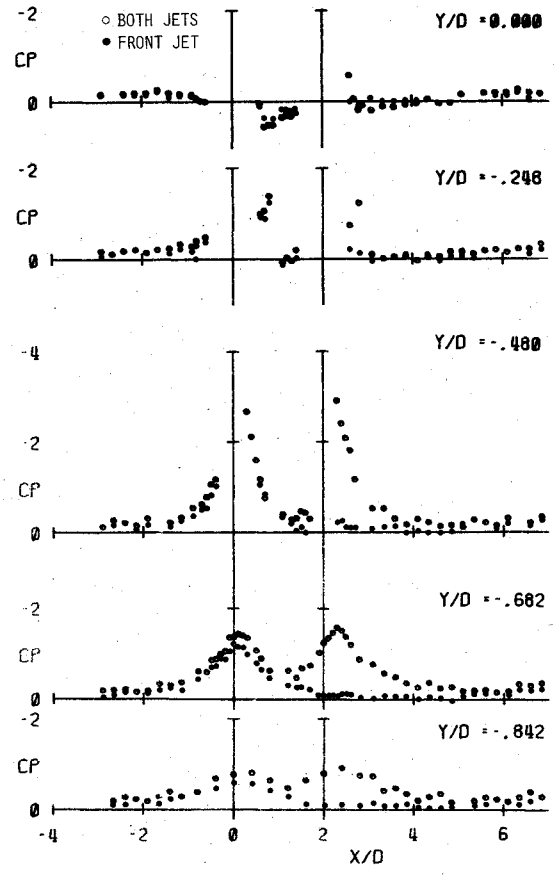

Fig. 11 Surface pressure distribution (ΔC_p): 75 deg, $R=8$, $S/D=2$, and flat-top exit.

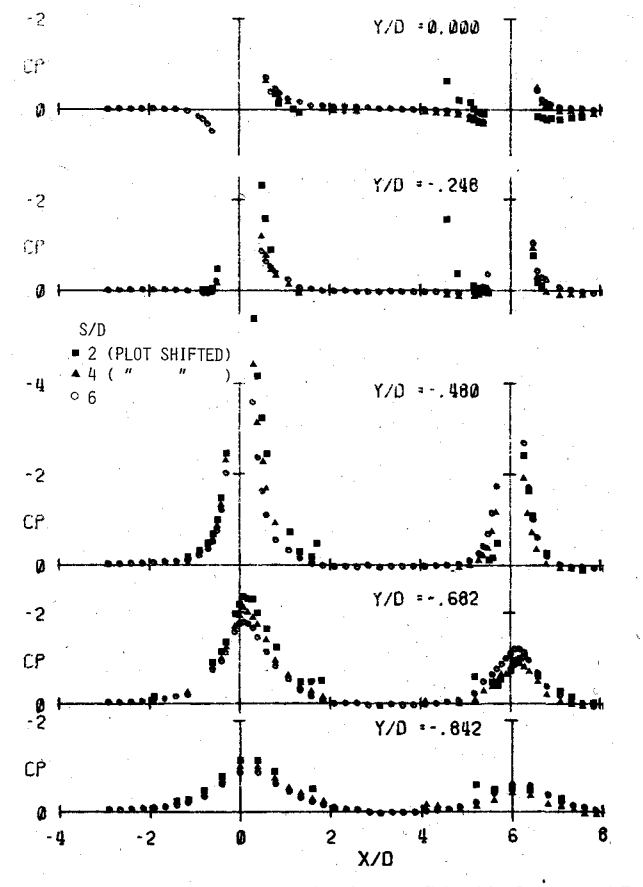

Fig. 10 Surface pressure distribution (ΔC_p): 90 deg, $R=4.7$, $S/D=2$, 4, and 6, and contoured exit.

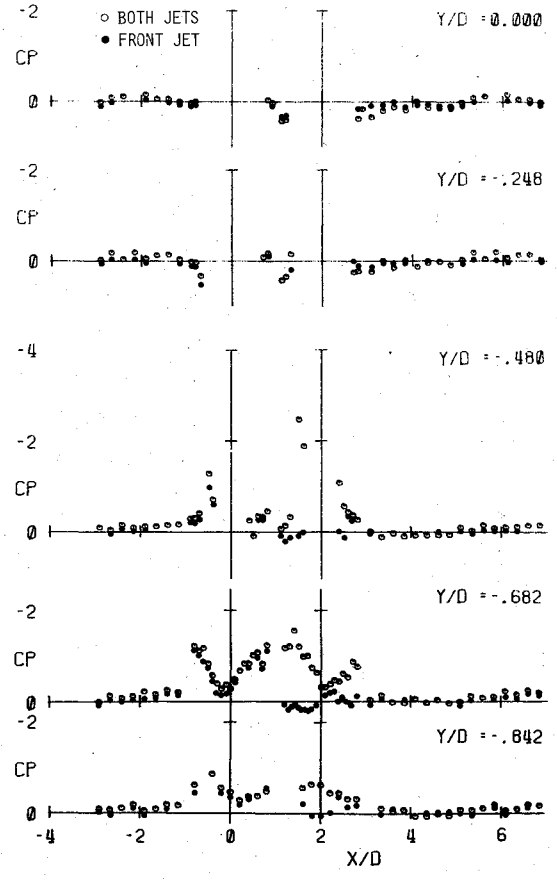

Fig. 12 Surface pressure distribution (ΔC_p): 60 deg, $R=8$, $S/D=2$, and flat-top exit.

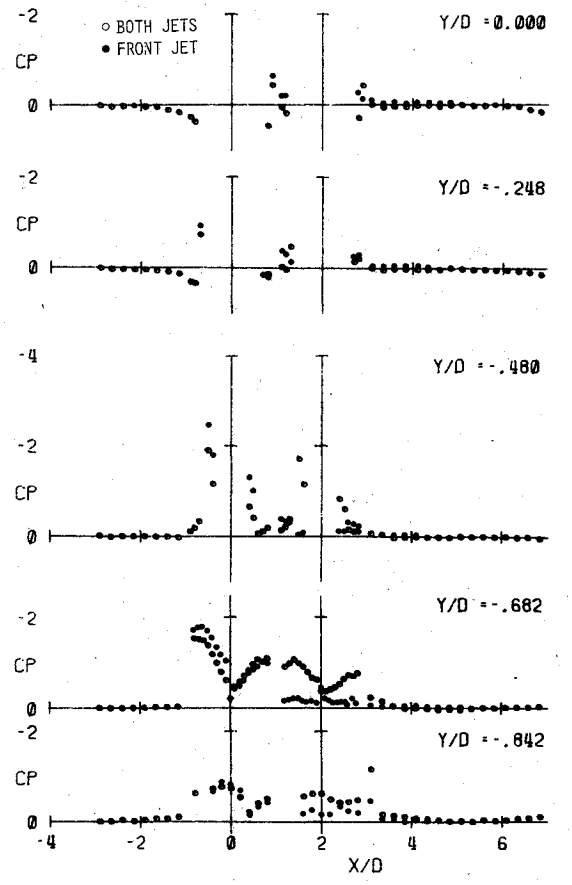

Fig. 13 Surface pressure distribution (ΔC_p): 60 deg, $R=4$, $S/D=2$, and flat-top exit.

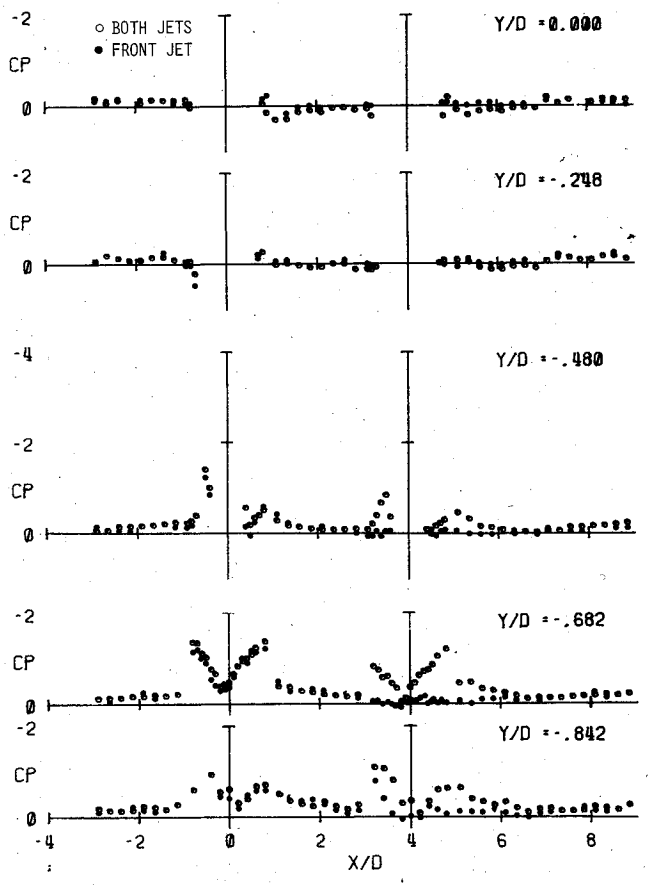

Fig. 14 Surface pressure distribution (ΔC_p): 60 deg, $R=8$, $S/D=4$, and flat-top exit.

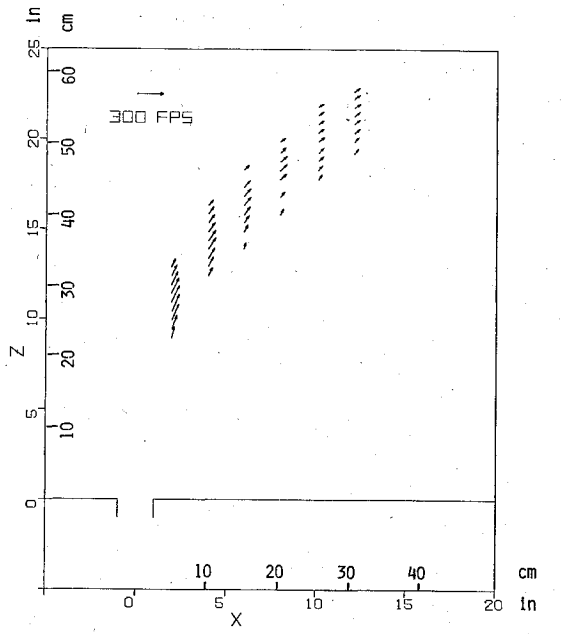

Fig. 15 Velocity vector data in the jet: 90 deg, $R=6.5$, front nozzle only.

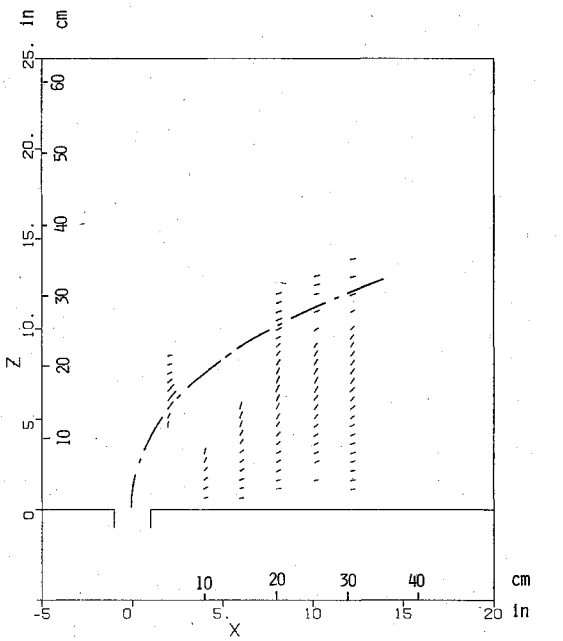

Fig. 16 Velocity vector data: 90 deg, $R=3.2$, front nozzle only and comparison of trajectory prediction with analysis of Ref. 28.

flow direction. The dual-jet results show that the influence of the rear jet is less than that of the front jet at this close spacing. On the other hand, the presence of the rear jet seems to strengthen the influence of the front jet slightly. An appreciation of the right/left symmetry found can be gained from the transverse variations plotted in Fig. 4 for this same case.

The effect of the important parameter $R=V_j/V_\infty$ is illustrated by the data in Fig. 5 for $R=3.2$ at 90 deg with a contoured exit. The patterns are quite similar to those for $R=7.7$ in Fig. 3; however, one must recall that C_p denotes the pressure difference Δp normalized with the freestream dynamic pressure, which is different for the two cases. The differences in ΔC_p are largest with increasing lateral distance and in the vicinity of the second jet.

The possible influence of different Reynolds numbers based on length along the body to the first jet at the same dimen-

sionless velocity ratio R was studied by running some tests at the same R but different V_∞. Some results are shown in Fig. 6. This particular case showed an influence larger than usually was found, and the effect is generally seen to be rather small.

Another variable considered in these tests was the geometry of the nozzle exit. The results presented so far correspond to the presumably simplest case of the nozzle exits contoured to the curved body surface. In Figs. 7 and 8 results for a flat-topped nozzle at $R=8$ and $R=3$, 90 deg, and $S/D=2$ are given, and these may be compared to the contoured nozzle results in Figs. 3 and 5. As might be expected, there are large effects between the nozzles. Also, the magnitude of the largest (absolute values) ΔC_p is reduced, and the lateral decay seems faster. Lastly, the influence of exit geometry is found to be larger at the higher velocity ratio.

The results of increasing S/D to 4.0 and then 6.0 at 90 deg with a contoured nozzle exit are shown in Figs. 9 and 10 for $R=4.7$. The results in Fig. 9 show that the rear jet is still strongly "sheltered" by the front jet at $S/D=4.0$. Now, however, the presence of the rear jet slightly reduces the influence of the front jet as opposed to the results for $S/D=2.0$. The data presented in Fig. 10 are for both jets operating at $R=4.7$, 90 deg with contoured injectors at $S/D=2.0$, 4.0, and 6.0. Note that the data for the lesser spacings have been "shifted" downstream to overlay the $S/D=6.0$ data for the rear nozzle. Here, one can see that the influence of the rear on the front jet is reduced from 2.0 to 4.0 to 6.0. The pattern in front of the rear jet changes sharply with S/D from 2.0 to 4.0, but only slightly from 4.0 to 6.0.

The influence of injection angle for flat-topped nozzles is displayed in Figs. 11-14. The results in Fig. 11 for $R=8$ and $S/D=2.0$ at 75 deg can be compared with those in Fig. 7 for 90 deg. The peak values near the front jet are increased slightly and those near the rear jet are increased more, especially at greater lateral distances. The ΔC_p values between the jets tend to be slightly more negative. The general trends continue for the 60 deg case in Fig. 12, but a new feature also appears. A "peak and valley" pattern appears next to the jets. This is very pronounced at $y/D=0.682$ near the front jet. This pattern was not observed at 90 or 75 deg. The same pattern is seen in Fig. 13 for $R\approx 4$ at 60 deg. At this lower velocity ratio, the rear jet decreases the influence of the front jet on the body surface. For all of the inclined jet cases, the influence of each jet is about the same, indicating that there is little "sheltering" even at this close $S/D=2.0$. This behavior is clearest at the higher R.

The effect of increased spacing to $S/D=4.0$ for the inclined jets is shown in Fig. 14 for $R=8$ at 60 deg. The "peak and valley" pattern is repeated, and the influence of the rear jet on the front and vice versa is slight.

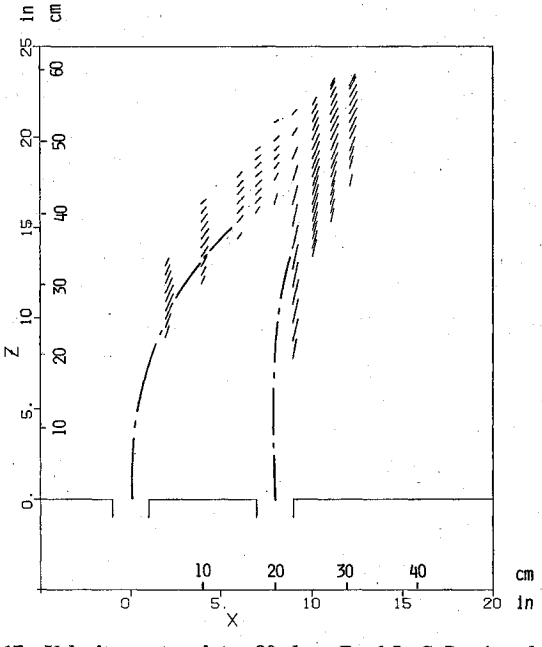

Fig. 17 Velocity vector data: 90 deg, $R=6.5$, $S/D=4$ and comparison of trajectory prediction with analysis of Ref. 28.

Flowfield Measurements

To amplify on the surface pressure data, some limited measurements of the jet flowfield above the surface were made with the yawhead probe. A plot of the local velocity vectors in the plane of the jets for $R=6.5$ at 90 deg is shown in Fig. 15 for injection from the front nozzle alone. The trajectory of the jet can be seen, and the high penetration across the main flow is clear. The same type of presentation for $R=3.2$ in Fig. 16 shows the sharply reduced penetration that results. The intersection region with two jets at $R=6.5$ is displayed in Fig. 17. Once can observe that the rear jet is strongly "sheltered" by the front jet; the trajectory of the rear jet is nearly vertical until the intersection.

The ability of the simple analysis of Ref. 28 to predict the trajectory of single and dual jets at various velocity ratios is demonstrated for two cases in Figs. 16 and 17. Obviously, the main features of the flow are predicted accurately.

Discussion

Some of the main conclusions that were found and presented earlier can be summarized as follows. First, the maximum (negative) value of ΔC_p decays faster with arc length around the body than with spanwise distance on a flat plate. Second, the effects of a flat-top nozzle as opposed to a contoured exit are large between the two nozzles. Also, the magnitude of the largest ΔC_p values is reduced. Third, the rear jet is strongly sheltered by the front jet, producing lower ΔC_p values near the rear jet. Finally, the ΔC_p pattern near the jets is strongly influenced by injection angle.

Flowfield measurements were made for a few cases in the test matrix. It was shown that a simple integral analysis can be used to provide good predictions of the jet trajectories before intersection.

Acknowledgment

This work was supported under NASA Grant NAS2-10437.

References

[1]Schetz, J. A., *Progress in Astronautics and Aeronautics —Injection and Mixing in Turbulent Flow,* Vol. 69, AIAA, New York, 1980.

[2]Vogler, R. D., "Surface Pressure Distributions Induced on a Flat Plate by a Cold Air Jet Issuing Perpendicularly from the Plate and Normal to a Low-Speed Free-Stream Flow," NASA TN D-1629, 1963.

[3]Vogler, R. D., "Interference Effects of Single and Multiple Round or Slotted Jets on a VTOL Model in Transition," NASA TN D-2380, Aug. 1964.

[4]Bradbury, L. J. S. and Wood, M. N., "The Static Pressure Distributions Around a Circular Jet Exhausting Normally From a Plane Wall Into an Airstream," British. Aeronautical Research Council, C.P. 822, 1965.

[5]Margason, R. J., "Jet-Induced Effects in Transition Flight. Conference on V/STOL and STOL Aircraft," NASA SP-116, 1966, pp. 177-189.

[6]Gentry, C. L. and Margason, R. J., "Jet Induced Lift Losses on VTOL Configurations Hovering In and Out of Ground Effect," NASA TN D-3166, Feb. 1966.

[7]Soullier, A., "Testing at SI. MAS for Basic Investigation on Jet Interactions. Distributions of Pressures Around the Jet Orifice," NASA TTF-14066, April 1968.

[8]Fricke, L. B., Wooler, P.T., and Ziegler, H., "A Wind Tunnel Investigation of Jets Exhausting Into a Crossflow," USAF, AFFDL-TR-70-154, Vols. I-IV, Dec. 1970.

[9]Margason, R. J., "Review of Propulsion-Induced Effects on Aerodynamics of Jet/STOL Aircraft," NASA TN D-5617, Feb. 1970.

[10]Fearn, R. L. and Weston, R. P., "Induced Pressure Distribution of a Jet in a Crossflow," NASA TN D-7916, June 1975.

[11] Taylor, P., "An Investigation of an Inclined Jet in a Crosswind," *Aeronautical Quarterly,* Vol. XXVIII, Part I, Feb. 1977, pp. 51-58.

[12] Kuhlman, J. M., Ousterhout, D. S., and Warcup, R.W., "Experimental Investigation of Effects of Jet Decay Rate on Jet-Induced Pressures on a Flat Plate," Tabulated Data, NASA CR-158990, Nov. 1978.

[13] Lee, C. C., "A Review of Research on the Interaction of a Jet With an External Stream, Tech," Brown Engineering Co., Inc., Research Lab. Note R-184, (Contract No. DA-01=021-AMC-11528 (z)), March 1966. (Available from Defense Documentation Center as AD 630 294.)

[14] Garner, J. E., "A Review of Jet Efflux Studies Application to V/STOL Aircraft," USAF, AEDC-TR-67-163, Sept. 1967. (Available from Defense Documentation Center as AD 658 432.)

[15] Perkins, S. C. Jr. and Mendenhall, M. R., "A Study of Real Jet Effects on the Surface Pressure Distribution Induced by a Jet in a Crossflow," NASA CR-166150, March 1981.

[16] Margason, R. J., "The Path of a Jet Directed at Large Angles to a Subsonic Freestream," NASA TN D-4919, Nov. 1968.

[17] Ziegler, H. and Wooler, P. T., "Analysis of Stratified and Closely Spaced Jets Exhausting into a Crossflow," NASA CR-132297, Nov. 1973.

[18] Ousterhout, D. S., "An Experimental Investigation of a Cold Jet Emitting from a Body of Revolution into a Subsonic Free Stream," NASA CR-2089, July 1972.

[19] Abramovich, G. N., *The Theory of Turbulent Jets,* MIT Press, Cambridge, Mass., 1963, pp. 541-552.

[20] Wu, J. C. and Wright, M. A., "A Blockage-Sink Representation of Jet Interference Effects for Noncircular Jet Orifices. Analysis of a Jet in a Subsonic Crosswind," NASA SP-218, 1969, pp. 85-99.

[21] Street, T. A. and Spring, D. J., "Experimental Reaction Jet Effects at Subsonic Speeds. Analysis of a Jet in a Subsonic Crosswind," NASA SP-218, 1969, pp. 63-83.

[22] Dietz, W. E. Jr., "A Method for Calculating the Induced Pressure Distribution Associated with a Jet in a Crossflow," M. S. Thesis, Florida Univ., 1975 (also available as NASA CR 146434, 1975).

[23] Yen, K. T., "The Aerodynamics of a Jet in a Crossflow," NADC-78291-60, Dec. 1978.

[24] Perkins, S. C. Jr. and Mendenhall, M. R., "A Correlation Method to Predict the Surface Pressure Distribution on an Infinite Plate or a Body of Revolution from which a Jet is Issuing," NASA CR 152345, Jan. 1980.

[25] Fearn, R. L., Kalota, C., and Dietz, W. E. Jr., "A Jet Aerodynamic Surface Interference Model," *Proceedings, V/STOL Aircraft Aerodynamics,* Vol. 1, Naval Postgraduate School, Monterey, Calif., May 1979.

[26] Campbell, J. F. and Schetz, J. A., "Analysis of the Injection of a Heated Turbulent Jet into a Cross Flow," NASA TR R-413, Dec. 1973.

[27] Baker, A. J., Manhardt, P. E., and Orzechowski, J. A., "A Three-Dimensional Finite Element Algorithm for Prediction of V/STOL Jet-Induced Flowfields," AGARD Symposium, Lisbon, Portugal, Nov. 1981.

[28] Isaac, K. M. and Schetz, J. A., "Analysis of Multiple Jets in a Cross-Flow," ASME Paper 82-WA/FE-4, Nov. 1982.

[29] "7×10 Wind Tunnel Guide," NASA Ames Research Center, Oct. 1978.

[30] Schetz, J. A., Lee, H., and Kong, F., "Mean and Turbulent Flow Measurements in the Near-Wake Region of a Self-Propelled Submarine- and/or Airship-Like Model at Pitch or Yaw," VPI-Aero-097, Sept. 1979.